LA-UR 94-4084

Conf-941144--2

Los Alamos National Laboratory is operated by the University of California for the United States Department of Energy under contract W-7405-ENG-36

TITLE: "Deformation of C15 Laves Phase Alloys"

AUTHOR(S): Fuming Chu, D. P. Pope

SUBMITTED TO: 1994 Annual Meeting of MRS
Boston, MA

DISCLAIMER

Los Alamos Los Alamos National Laboratory
Los Alamos, New Mexico 87545

FORM NO. 836 R4
ST. NO. 2629 5/81

DISCLAIMER

Portions of this document may be illegible in electronic image products. Images are produced from the best available original document.

Deformation of C15 Laves Phase Alloys

F. Chu* and D. P. Pope**

* Center for Materials Science, MS K765, Los Alamos National Laboratory, Los Alamos, NM 87545, U. S. A.

** Department of Materials Science and Engineering, University of Pennsylvania, Philadelphia, PA 19104, U. S. A.

ABSTRACT

Details of the structure and previous work on the deformation of C15 Laves phases are reviewed. The phase diagram of the Hf-V-Nb system, some metallurgical and physical properties, mechanical behavior, and the deformation mechanisms of HfV_2+Nb (C15 HfV_2+Nb and V-rich bcc solution) are presented based on our previous work. Theoretical approaches to understanding the results of these studies are discussed.

INTRODUCTION

If new intermetallic-based alloys are to be selected on the basis of low density and high melting temperature, as would be, for example, for use in rotating components in the hot sections of gas turbines, then the attraction of topologically close-packed (TCP) materials immediately becomes apparent. In this group of compounds the crystal structure is primarily determined by the ratio of the atomic sizes of the components such that they can most efficiently fill space (1-2). Such structures generally are complex, in that the unit cell contains many atoms, even though the crystal structure may have high symmetry (2). Within the category of TCP phases are the Laves phases (C14, C15 and C36), the A15 phase, the σ phase, the μ phase, the M phase, etc. (2). A number of these phases have quite high melting temperatures, low densities and contain substantial amounts of strong oxide formers, for example, $NbCr_2$ (C14/C15 Laves phases) (3-4) and $SiCr_3$ (A15 phase) (5). In this paper we review the mechanical properties of the cubic (C15) Laves phases, with special attention to HfV_2+Nb, because it shows some plastic deformability at low temperatures, unlike other C15 compounds (6-8).

C15 CRYSTAL STRUCTURE

The crystal structure of C15 is shown in Fig.1. The main geometric characteristic of the C15 structure, a type of topologically close-packed structure similar to geometrically close-packed metals, is the specific stacking sequence along the [111] direction. The C15 structure is constructed by an ··· **abcabc** ··· stacking sequence, where each of these symbols represents a four layer group instead of a single layer. In detail, the stacking sequence of (111) planes is given by:

$$\cdots\cdots \underbrace{\alpha A \alpha c}_{a} \underbrace{\beta B \beta a}_{b} \underbrace{\gamma C \gamma b}_{c} \cdots\cdots$$

In this sequence, the larger (A) atom always occupies the layers indicated by Greek letters and the small (B) atom occupies those indicated by Roman letters. The cubic C15 (3C) and hexagonal C14 (2H) phases are related in the same way as fcc and hcp structures, i.e., C15 is based on the ···**abcabc**··· stacking sequence while C14 is based on the ···**abab**··· stacking sequence (8, 9, 10).

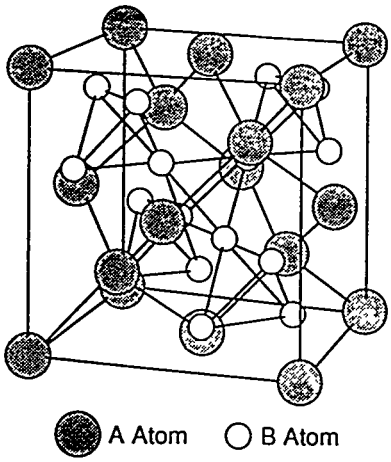

Fig. 1 C15 AB_2 crystal structure [Ref. (8)].

There are two kinds of sandwiches in this stacking sequence of (111) planes, αAα (βBβ and γCγ) and αcβ (βaγ and γbα), as shown in Fig. 2 (8). The packing in these sandwiches and the interlayer distances are quite different. The αAα type sandwiches are more widely spaced and appear to be quite rigid, primarily due to the larger shear vector and directional bonding between the larger atoms. Experimentally, stacking faults have not been observed between these layers (11). The αcβ type sandwiches are closely spaced and also more deformable, basically due to a shorter shear vector, and the corresponding stacking faults have been observed between those layers in TEM studies (11).

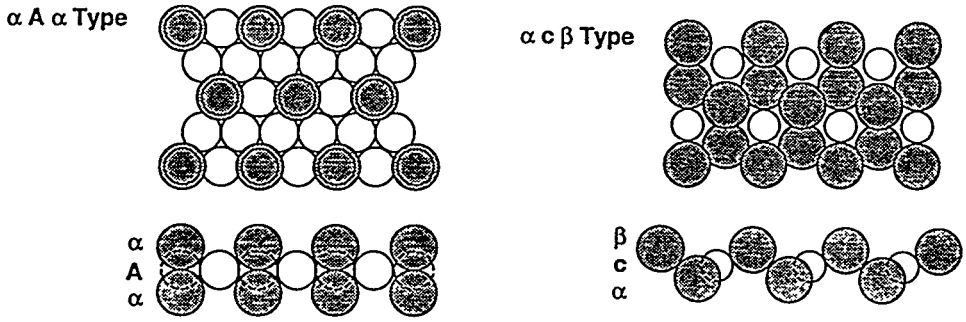

Fig. 2 The two kinds of sandwiches in the stacking sequence of (111) planes, αAα (βBβ and γCγ) and αcβ (βaγ and γbα) [Ref. (8)].

The geometric characteristics of the crystal structure appear to have the largest influence on the deformation behavior of C15 intermetallic compounds. To increase the deformability of a C15 material, the deformability of αcβ type sandwiches must be increased, say by alloying with the proper ternary element.

REVIEW OF PREVIOUS WORK

A number of studies of the mechanical properties of C15 compounds have been carried out in recent years. The most significant, for purposes of this study, are listed below: Allen, Delanignette and Amelinckx (11) deformed $TiCr_2$ and $TiCo_2$ and observed 1/6<112> stacking faults only on αcβ-type sandwiches, thereby supporting the synchroshear mechanism (more

about this later). Moran (12) showed that plasticity is carried by {111}(110) slip in $MgCu_2$ at high temperatures ($T>0.65T_m$), and continued by Livingston, Halland, and Koch (13).

The most significant recent results on a C15 Laves phase are those of Livingston and Hall (7). They based their work on earlier work which showed that a Hf-V-Nb alloy with a HfV_2-based C15 phase matrix can be cold-rolled by as much as 30% at room temperature (6). Livingston and Hall showed, using TEM and HREM, that this deformation is accomplished primarily by the production of $\{111\}/<11\bar{2}>$ mechanical twins.

Based on this work, we studied the phase equilibria, metallurgical and physical properties, mechanical behavior, and deformation mechanisms of the C15 Laves phase in the Hf-V-Nb system.

PHASE DIAGRAM OF THE Hf-V-Nb SYSTEM

Given the dramatic affects of Nb on twinning in C15 HfV_2, we determined the phase diagram (14), especially the regions of stability of the C14 and C15 Laves phases in this alloy as shown in Fig. 3.

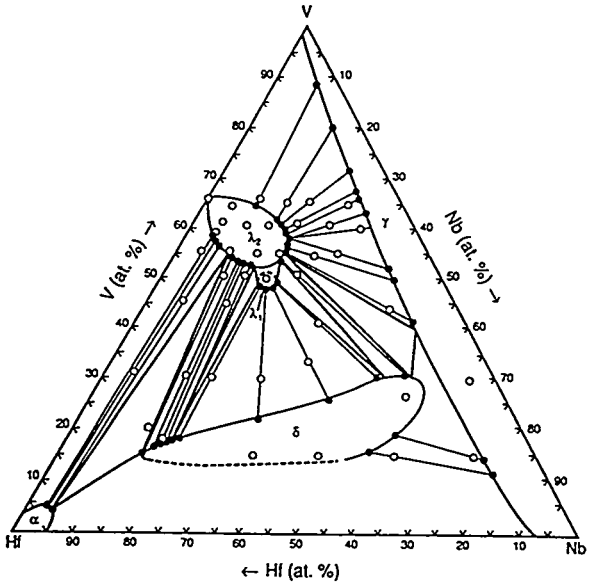

Fig. 3 The Hf-V-Nb equilibrium phase diagram at 1000°C. o : composition tested; • : composition of each phase; —— : tie-lines; ▬▬ : established phase boundaries; ▪▪▪▪ : approximate phase boundaries. λ_2 = C15; λ_1 = C14 ; γ = b.c.c. solid solution; δ = b.c.c. solid solution [Ref. (14)].

The extent of the cubic Laves phase field (λ_2) based on C15 HfV_2 at 1000°C is relatively large, with a compositional range of 0 to 20 at.% Nb. A previously-unknown ternary C14 hexagonal Laves phase field (λ_1) has been found but it is small relative to the C15 field. There is a b.c.c. disordered phase region at 1000°C in the Hf-V-Nb alloy at low V concentrations. Some of the equilibrium phase relations of the Hf-V-Nb system at 1000°C have been established.

From the phase diagram it can be seen that there may be a two phase field with C15 and C14 Laves phases in equilibrium. This suggests that for compositions near the cubic-hexagonal transition, a stress-assisted martensitic transformation might be possible, perhaps yielding a

form of "transformation ductility or toughening". It is also possible that the C15 Laves phase may continuously change to the C14 Laves phase with increasing Nb contents (15).

It can also be seen from Fig. 3 that there are some phase fields where the C15 intermetallic is in equilibrium with solid solutions, for example, the twinned samples examined by Livingston and Hall (7) came from the λ_2,γ phase field. The existence of the ductile bcc phase appears to be very important for allowing twinning of the C15 phase prior to fracture (8).

METALLURGICAL AND PHYSICAL PROPERTIES OF C15 HfV_2+Nb

The mechanical behavior of a material usually is intimately related to its metallurgical and physical properties. Consequently, in addition to the study of the deformation of C15 HfV_2+Nb, we also investigated some relevant metallurgical and physical properties, for example, thermal properties (16), phase stability at both low and high temperatures (16-17), and elastic properties (17-18). It was found that while the coefficient of thermal expansion of the alloy is quite low, the average amplitude of the atomic thermal vibrations becomes very large as the temperature increases. It was also found that C15 HfV_2 is stable from up to 1073K, but it undergoes a structural transformation at 115K. Furthermore, alloying HfV_2 with Nb stabilizes the C15 structure at low temperatures. It was also found that the elastic properties of both binary C15 HfV_2 and ternary C15 HfV_2+Nb phases show anomalous temperature dependence , i.e., the shear and Young's moduli increase with increasing temperature, the bulk modulus is virtually constant, and the Poisson's ratio is higher than observed for most materials, and it decreases with increasing temperature.

These results are very helpful in understanding the mechanical behavior and deformation mechanisms of the C15 Laves phases

MECHANICAL BEHAVIOR OF THE C15 HfV_2+Nb

The single phase λ_2 alloys prepared in the course of determining the isothermal section in Fig. 3 showed substantially different degrees of brittleness, as indicated by sensitivity to thermal shock and handling stresses. Those alloys with V/Hf>2 and also containing substantial Nb additions appeared to be less brittle than those for which V/Hf<2.

In addition, two phase alloys having a C15 matrix and the V-rich bcc solid solution as the second phase appear more ductile if the composition of the C15 matrix is also in the V/Hf>2 region and also has a high Nb content. To investigate this effect we performed compressive tests on $Hf_{14}V_{64}Nb_{22}$, a two phase alloy consisting of a C15 Laves phase matrix with V/Hf>2 and a V-rich bcc solid solution second phase. The microstructure of this alloy is shown in Fig. 4.

Fig.4 Microstructure of $Hf_{14}V_{64}Nb_{22}$: the matrix is C15 HfV_2+Nb and the second phase is V-rich bcc solution.

Based on the stress-strain curves measured at a strain rate 8.4x10-4 s^{-1} and at different temperatures, the temperature dependence of the yield stress (σ_Y), UTS, fracture stress(σ_F) and plastic strain (ε_{pl}) were obtained, as shown in Fig. 5. As seen in Fig. 5, the mechanical behavior of the C15+bcc alloy can be divided into three distinct temperature regions. In the low temperature region, from room temperature to 300°C, the alloy is fairly ductile; in the medium temperature region, from 300°C to 750°C, the alloy exhibits a ductility minimum; and at high temperatures ($T>0.65T_m$), the alloy shows large plastic deformations [Ref. (16)].

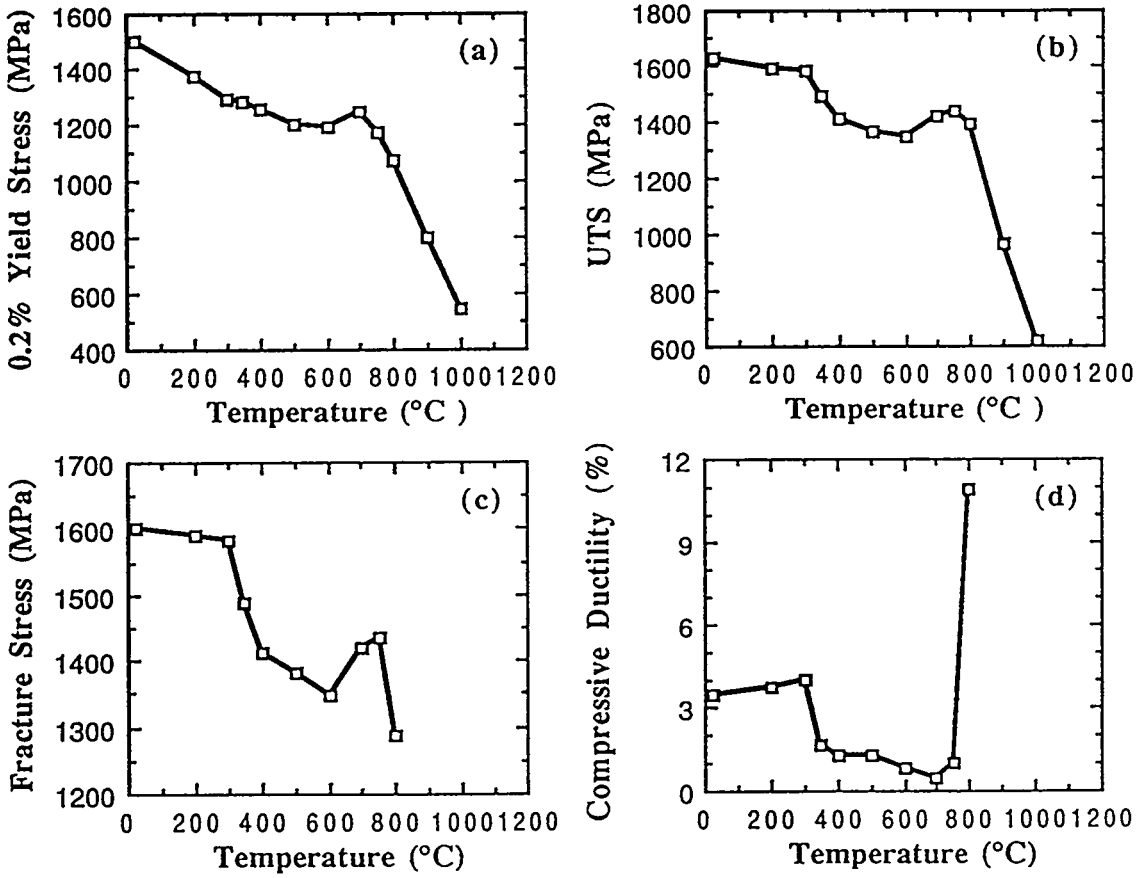

Fig.5 Plots of (a) σ_Y, (b) UTS, (c) σ_F and (d) ε_{pl} vs. temperature for $Hf_{14}V_{64}Nb_{22}$ [Ref. (16)].

Well-preserved surfaces of the two phase samples tested at room temperature were examined using optical and scanning electron microscopy up to 10,000x. No slip traces were found in the C15 phase. TEM examination of the sample showed that the major deformation mode in the ternary C15 Laves phase is mechanical twinning, as shown in Fig. 6. The bands were identified to be $\{111\}/\langle 11\bar{2}\rangle$ twins, the one commonly seen in fcc materials (20-21), and the same one observed by Livingston and Hall (7). TEM observations of the samples tested in the intermediate temperature region, ranging from 300°C to 750°C, showed that the frequency of deformation twinning in the C15 phase substantially decreases with increasing temperature in this temperature range.

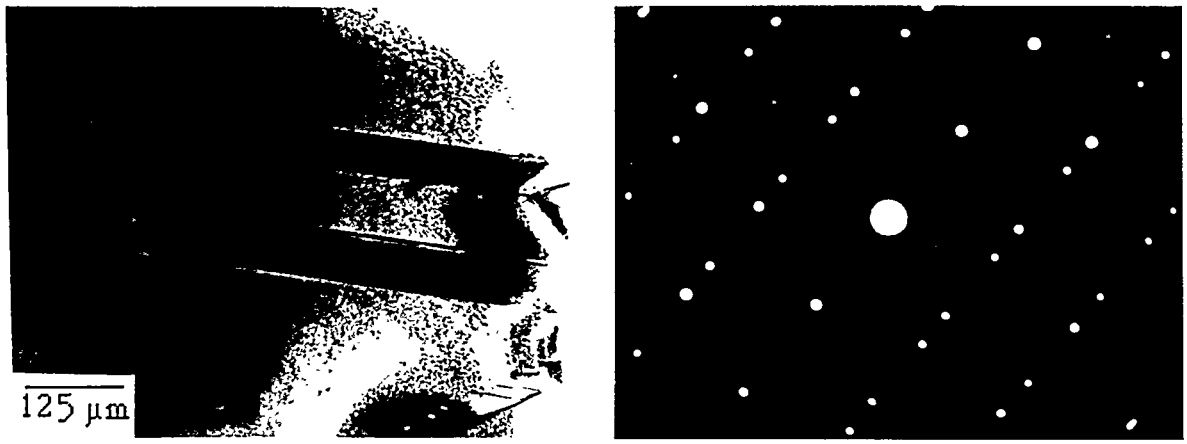

(a) (b)

Fig. 6 (a) Microstructure of a plastically deformed C15 alloy. The zone axis is [110]; twin interface is $(1\bar{1}1)$. (b) <110> diffraction pattern of $\{111\}\langle 11\bar{2}\rangle$ twin in this system [Ref. (8)].

The major deformation mode in the C15 phase at high temperatures ($T>0.65T_m$) is **b**=1/2<110> dislocation slip. The slip plane was not determined but presumably is {111}. These results are consistent with high temperature deformation studies of other cubic Laves phases by Moran (12) and Livingston et al. (13).

C15 DEFORMATION MECHANISMS

(1) Low Temperature C15 Twinning

Why do Nb additions increase the amount of twinning at room temperature? Why is Nb more effective in the region where V/Hf >2? Why does the frequency of twinning decrease at higher temperatures? These observations are all self-consistent if it is assumed that twinning of the C15 phase occurs by synchroshear of selected αcβ layers of the structure, as discussed below.

In the more complex twinning modes, most frequently occurring in superlattices, a simple homogeneous shear displaces only a fraction of the atoms of the crystal directly to positions appropriate to the twinned structure, and therefore 'shuffles' of the remaining atoms are hypothetically required to restore the original crystal structure (20-22). In this case, another element, the percent of atoms undergoing this shuffling, is needed for completely describing the twinning process. A small percent of shuffling atoms suggests a shuffling mechanism which may not be too difficult. Generally speaking, twins in some simple metals (particularly bcc) and most complex superlattices involve long shear vectors, and/or atomic shuffling, if the shear is assumed to be homogeneous, as it is in the usual treatment.

However, $\{111\}\langle 11\bar{2}\rangle$ twinning may be accomplished in the C15 structure without long shear vectors and without shuffles. A schematic representation of this process is shown in Fig. 7. Non-homogeneous synchroshear, occurring in each αcβ sandwich, transforms the matrix into a twin with no need for shuffles.

In synchroshear the smaller atoms in the deformable sandwich move in the sequence of c → b → a → c, and the stable sandwiches glide following the order of βB β → γC γ → αAα → βB β. The schematic representation of synchroshear occurring in each αcβ sandwich in C15 is shown in Fig. 7. The formation of twins is shown below [Ref. (8)].

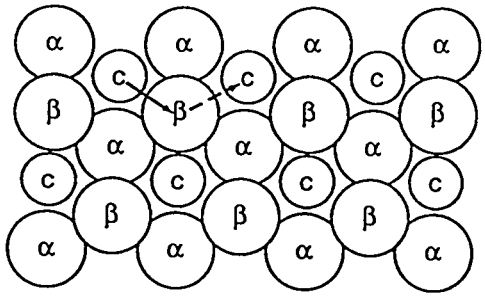

Fig. 7 Schematic representation of synchroshear.

··· α A α c β B β a γ C γ b α A | α c β B β a γ C γ b α A α c β B β ...
··· α A α c β B β a γ C γ b α A | α b γ C γ b α A α c β B β a γ C γ b ...
··· α A α c β B β a γ C γ b α A | α b γ C γ a β B β a γ C γ b α A α c ...
··· α A α c β B β a γ C γ b α A | α b γ C γ a β B β c α A α c β B β a ...
Matrix → | ←Twin

Synchroshear and twinning in the C15 phases could also be accomplished by the motion of synchro-Shockley partials and zonal dislocations (11, 23, 24).

Why does Nb alloying promote twinning? Considering the large differences in coordination and size between the constituent elements in the AB_2 C15 structure , we assume that when we add an element C of intermediate atomic size ($r_B < r_C < r_A$) there are no substantial amount of anti-site defects (A⇔B) are produced in the equilibrium state. Otherwise, there would be a large local stress field and a high defect energy, primarily due to the large size difference and special coordination situations of A and B atoms in the topologically close-packed structure. In addition, from an analysis of the A and B coordinations, it can be seen that each A (or B) atom is geometrically identical with identical coordination situations. Thus, when C atoms are added, it is most likely that C randomly occupies both A and B sites according to the stoichiometry, so that A atoms always occupy A sites , B atoms occupy B sites, and C atoms occupy both A and B sites in such a way as to satisfy stoichiometry. So the rule that emerges for substitution is that A atoms still occupy A sites, B atoms still occupy B sites and C atoms occupy both A sites and B sites in a ratio that satisfies stoichiometry [8, 25, 26].

To check this hypothesis, we measured the x-ray powder diffraction patterns for several compositions and compared them to the predicted intensities, based on the above assumptions. The results agreed remarkably well. We therefore conclude that Nb substitutes in C15 HfV_2 as described above.

Ternary alloying element substitutes can have a strong influence on the mechanical properties of C15 intermetallics in the following way: Geometrically, from an analysis of the stacking sequence and the two kinds of sandwiches (αAα and αcβ) in the C15 structure, our assumptions about site occupancy provides insights into fault energies. If V/Hf=2 in a ternary Hf-V-Nb alloy, then the ratios of Nb/V on V sites and Nb/Hf on Hf sites are equal, based on

the above assumptions. If V/Hf < 2, a larger fraction of V sites is occupied by Nb and if V/Hf > 2 then a larger fraction of Hf sites are occupied. As more Nb occupies Hf sites, the free volume in the structure increases, since $r_{Nb}<r_{Hf}$, and since the αcβ sandwiches contain disproportionally more Hf sites than αAα sandwiches. Therefore αcβ sandwiches have the larger free volume. This extra free volume is expected to facilitate synchroshear in this type of sandwich.

As further evidence for the importance of synchroshear in C15 compounds, we found extensive faceting of Σ3(<110>/70.53°) tilt grain boundaries (27). Other grain boundaries remain unfaceted. The Σ3(<110>/70.53°) tilt grain boundaries form facets of the type $\{111\}_1/\{111\}_2$, $\{112\}_1/\{112\}_2$, $\{001\}_1/\{221\}_2$, and $\{111\}_1/\{115\}_2$ with a marked preference for $\{111\}_1/\{111\}_2$. No other facets were observed. The $\{111\}_1/\{115\}_2$ facets can dissociate into a combination of $\{111\}_1/\{111\}_2$ and $\{112\}_1/\{112\}_2$ facets. Annealing twins of the type {111}<112> also form in the C15 alloy by the anisotropic migration along the <112> direction of boundary facets with $\Sigma3\{112\}_1/\{112\}_2$ interfaces, resulting in the accumulation of $\{111\}_1/\{111\}_2$ facets at high temperatures. A dislocation model was proposed to explain this process, that involves synchro-Shockley partial dislocation triplets gliding via the synchroshear mechanism. That is, the annealing twins grow via a ledge mechanism.

(2) Ductility Drop in Intermediate Temperatures

The ductility drop in the intermediate temperature region is due to the lack of mechanical twinning in the C15 Laves phase. There are several possible reasons for this: segregation of impurity atoms, oxidation, a phase transformation, and changes in thermal properties. The first possibility can be ruled out because failure is almost entirely by cleavage, not intergranular, and therefore impurity segregation is not important. Oxidation, or other environmental factors, were ruled out by testing in a 10^{-6} Torr vacuum, and a phase transformation was ruled out by performing high temperature x-ray diffraction experiments (24). Only thermal properties remain. The high temperature x-ray diffraction studies showed that, while the coefficient of thermal expansion of the alloy is quite low, the average amplitude of the atomic thermal vibrations becomes very large as the temperature increases, as mentioned above. Such a combination gives rise to increasingly large interferences between the atoms in the αcβ sandwiches, resulting in reduced amounts of synchroshear and reduced amounts of twinning (24).

(3) High Temperature Dislocation Slip

The deformation mechanisms for the high temperature dislocation slip are not clear at present. TEM and HREM studies are needed to investigate the slip plane, Burgers vector, dissociation, and core structure of the dislocations in single crystal specimens.

THEORETICAL APPROACH

In order to optimize the properties of C15 intermetallic compounds, it is necessary to understand these experimental results and obtain additional theoretical information which is

difficult to access by experiments. The achievement of this goal depends strongly on a thorough understanding of the electronic and mechanical properties of the materials, and this can be accomplished by a combination of first-principle calculations and atomistic simulations (28,29).

Some first-principle calculations have previously been performed on several systems in the course of studies of magnetism and superconductivity in C15 compounds, e.g., ZrV_2 (30), $MgZn_2$ (31), $ZrZn_2$ (32), $LaAl_2$, $LuAl_2$ and YAl_2 (33), and $MgCu_2$, $MgZn_2$ and $MgNi_2$ (34), AFe_2 (A=Sc, Ti, V; Y, Zr, Nb; and Lu, Hf, Ta) (35), and AB_2 (A= IIIA-VA transition metal elements, B=VIA-VIIIA transition metal elements) (36). Recently, some simple calculation schemes were used to study the structural stability of Lave phases , e.g., a model potential was employed to investigate the structural stability of C14 $MgZn_2$ (37), the tight-bonding d-bond model was used to investigate the transition metal Laves phase stability among three competing phases (C15, $C11_b$ and C16) (38), extended Huckel band calculations were performed on model AB_2 compounds to study the relative stability of C14 and C15 phases (39), and the more realistic tight-bonding formalism was employed to examine the relationship between the three Laves phases (C14, C15 and C36) in the Ti-V and Ti-Cr systems (40). However, these studies were not extended to the investigations of the phase stability in the sense of alloying effect and ternary phase field.

Based on these investigations, it is clear that extensive first-principle calculations of total energy and electronic structure are needed for:

(a) Early transition metal (A and B=IVA-VIA transition metal elements)) Laves phases, because these refractory element-containing phases have high melting temperatures and therefore are potential high temperature structural materials;

(b) Basic physical parameters (e.g., lattice parameter, elastic constants, cohesive energy, and heat of formation,.) and metallurgical and physical properties (e.g., elastic properties, phase stability and alloying effects, solubility range, defect mechanisms, and structural transformations), because these quantities and properties are closely related the mechanical behavior and deformation mechanisms of the materials.

The linear muffin-tin orbital method with the atomic sphere approximation (LMTO.ASA) and the full potential linear muffin-tin method (LMTO.FP) have been used to investigate the basic physical parameters and metallurgical and physical properties of two C15 Laves phases: HfV_2 (17, 41) and $NbCr_2$ (42, 43). Some basic physical parameters, e.g., lattice parameters and elastic constants obtained from these calculations agree with the experimental data very well. We also obtained some quantities from these calculations , e.g., cohesive energy and heat of formation, which are very important but difficult to access from the available experimental data.

The electronic structures (band structures, density of states, and Fermi surfaces) obtained from these calculation were then used to explain some metallurgical and physical properties of the materials, e.g.:

(1) The phase stability (ternary C15 phase field) and the effects of alloying. These calculations showed that in addition to the geometric factors, the density of states at the Fermi level, $N(E_f)$, and the occupancy of bonding and anti-bonding d-states of C15 AB_2 play important roles in determining the ternary C15 phase field. This argument can be successfully used to explain the expansion of the ternary C15 phase field in Fig. 3.

(2) The temperature dependence of elastic properties of C15 AB_2. It was found that there are doubly degenerate electronic energy levels with a linear dispersion relation at the X-point of the irreducible Brillouin zone (IBZ). The temperature dependence of the electronic contribution to the shear modulus, c'_{44}, depends on the energy gap, $\Delta\varepsilon$, between this double degeneracy and the Fermi level. If $\Delta\varepsilon$ is small, the temperature dependence of c'_{44} is anomalous, i.e. c'_{44} increases with increasing temperature, therefore the shear modulus of the material is anomalous. Otherwise, the material exhibits normal temperature dependence of shear modulus.

(3) The low temperature structural stability of C15 AB_2. It was proposed that the low temperature structural instability of C15 HfV_2 and ZrV_2 is induced by phonon softening, resulting from a combination of a very large $N(E_f)$ and Fermi surface nesting. A small $N(E_f)$ and/or the absence of Fermi surface nesting can stabilize the C15 structure at low temperatures. This is supported by the fact that C15 TaV_2 is stable at low temperatures (17).

Future theoretical approaches may proceed along two directions: (a) first-principle calculations of defect energies of C15 Laves phases, e.g., stacking fault energies and twin boundary energies; (b) fitting of empirical atomic potentials using a combination of experimental and theoretical data (e.g., lattice parameter, elastic constants, and cohesive energy, etc.). Using these results, especially the interatomic potentials, we can simulate γ-surfaces, synchroshear, and dislocation core structures. This could be of benefit to understanding the mechanical behavior and deformation mechanisms of the C15 Laves phases.

CONCLUSIONS

1. An isothermal section for the Hf-V-Nb system has been established at 1000°C:
The extent of the cubic Laves phase based on HfV_2 is from 0 to 20 at. % Nb. The equilibrium phase region of the C14 hexagonal Laves phase has been located and is small relative to the C15 field. There are two b.c.c. disordered phases region at 1000°C, one at low V concentrations; and the other at low Hf concentrations. Some of the equilibrium phase relations of the Hf-V-Nb system at 1000°C have been established.

2. Some metallurgical and physical properties of C15 HfV_2+Nb have been investigated:
(a) The stability of the C15 Laves phase has been investigated. C15 HfV_2+Nb is thermally stable at high temperatures. Binary C15 HfV_2 is unstable at low temperatures. A structural phase transformation occurs at about 115K, but the resulting crystal structure has not yet been unambiguously determined. Alloying with Nb stabilizes the C15 structure.

(b) Anomalous elastic properties exist in both the binary and ternary C15 Laves phases. For ternary C15 compounds, the shear and Young's moduli increase with increasing temperature, the bulk modulus is virtually constant, and Poisson's ratio is very high and decreases with increasing temperature.

3. The mechanical behavior and deformation mechanisms of C15 HfV_2+Nb have been studied:

(a) Twinning is the major plastic deformation mode at low temperatures in C15 Hf-V-Nb alloys. The twinning occurs on {111} planes by shear in the <112> directions. This twinning mode can be accomplished via the synchroshear mechanism if the shear occurs on selected {111} planes, i.e. the shear is inhomogeneous. This mechanism involves only short displacements, 1/6<112>, and requires no atomic shuffles. The substitution of Nb into HfV_2 appears to facilitate deformation twinning by increasing the free volume in the planes undergoing synchroshear.

(b) The C15 alloy exhibits a ductility minimum in the intermediate temperature region (300°C-750°C). This is not the result of a phase transformation, but is probably caused by atomic interference across the (111) planes as a result of the low thermal expansion coefficient and relatively large atomic thermal vibrations which combine to inhibit synchroshear.

(c) The $Hf_{14}V_{64}Nb_{22}$ alloy exhibits good ductility above 800°C($T>0.65T_m$). The major deformation mode in this temperature regime is **b**=1/2<110> dislocation slip.

4. Total energy and electronic structure obtained from first-principle calculations can be used to explain and understand some of these experimental results.

ACKNOWLEDGMENT

F. Chu is supported by a Director-Funded Postdoctoral Fellowship at Los Alamos National Laboratory. This research is supported at the University of Pennsylvania by the Office of Naval Research (Grant No. N00014-91-J-1165).

REFERENCES

1. F. Laves, in *Theory of Alloy Phase*, p. 123, (ASM, Cleveland, OH), (1956).
2. J. H. Wernick, in Intermetallic Compounds, ed. by J. Westbrook, John-Wiley&Sons, Inc., New York, (1967).
3. M. Takeyama and C. T. Liu, Mater. Sci. & Eng., **A132**, 61 (1991).
4. D. J. Thoma and J. H. Perepezko, Mater. Sci. & Eng. **A156**, 97 (1992).
5. C. S. Chang, Ph. D. Thesis, University of Pennsylvania, (1991).
6. K. Inoue and K. Tachikawa, IEEE Trans. Mag. **Mag-13**, 840 (1977).
7. J. D. Livingston and E. L. Hall, J. Mater. Res. **5**, 5 (1990).
8. F. Chu and D. P. Pope, Mat. Sci. & Eng. **A170**, 39 (1993).
9. C. W. Allen and K. C. Liao, Phys. Stat. Sol. (a) **74**, 673 (1982).
10. P. M. Hezzledine, K. S. Kumar, D. B. Miracle and A. G. Jackson, Mat. Res. Soc. Symp. Proc. **288**, 591 (1992).

11. C. W. Allen, P. Delavignette and S. Amelinckx, Phys. Stat. Sol. (a) **9**, 237 (1972).
12. J. B. Moran, Trans. Metall. Soc. of AIME, **233**, 1473 (1965).
13. J. D. Livingston, E. L. Hall and E. F. Koch, Mat. Res. Soc. Symp. Proc. **133**, 243 (1989).
14. F. Chu and D. P. Pope, Scripta Met. et Mat. **26**, 399 (1992).
15. C. W. Allen: private communication, 1992.
16. F. Chu and D. P. Pope, Scripta Met. et Mat., **28**, 331, (1993).
17. F. Chu, T. ER. Mitchell, S. P. Chen, M. Šob, R. SIegl, and D. P. Pope, in this volume.
18. F. Chu, Ming Lei, A. Migliori, S. P. Chen, and T. E. Mitchell, Phil. Mag. B **70**, 867 (1994).
19. F. Chu and D. P. Pope, Mat. Res. Soc. Symp. Proc. Vol. **288**, 561 (1992).
20. J. W. Christian, *The Theory of Transformation in Metals and Alloys*, Pergamon Press, London, 1975.
21. J. W. Christian and D. E. Laughlin, Acta Metall. **36**, 1617 (1988).
22. M. Khantha, V. Vitek, and D. P. Pope, Mat. Res. Soc. Symp. Proc. **133**, (1989).
23. P. M. Hazzledine and P. Pirouz, Scr. Met. at Mat., **28**, 1277 (1993).
24. M. L. Kronberg, Acta Metall. **5**, 507 (1957).
25. F. Chu, Ph. D. Thesis, University of Pennsylvania, Philadelphia, PA, (1993).
26. D. P. Pope and F. Chu, in *Structural Intermetallics*, ed by R. Darolia, et al., 637, (TMS, Warrendale, PA), (1993).
27. D. P. Pope and F. Chu, Phil. Mag. A **69**, 409 (1994).
28. V. Vitek and S. P. Chen, Scripta Met. et Mat. **25**, 1237 (1991).
29. C. L. Fu and M. H. Yoo, Mater. Chem. & Phys., **32**, 25 (1992).
30. T. Jarlborg and A. J. Freeman, Phy. Rev. B, **22**, 2332 (1980).
31. P. Rennert and M. Taut, Phys. Status Solidi **41**, 703 (1970).
32. D. L. Johnson, Phys. Rev. B **9**, 2273 (1974).
33. A.C. Switendick, Proc. Rare Earth Res. Conf. 10th.
34. R. Haydock and R. L. Johannes, J. Phys. F **5**, 2055 (1975).
35. K. Terao and M. Shimizu, Phys. Stat. Sol. B 139, 485 (1987).
36. S. Asano and S. Ishida, J. Phys. F: Met. Phys. **18**, 501 (1988).
37. P. Rennert and A. M. Radwan, Phys. Stat. Sol. B **79**, 167 (1977).
38. Y. Ohta and D. G. Pettifor, J. Phys. Condens. Matter **2**, 8189 (1990).
39. R. L. Johnston and R. Hoffmann, Z. anorg. allg. Chem. **616**, 105 (1992).
40. M. Sluiter and P. E. A. Turchi, Phys. Rev. B **43**, 12521 (1991).
41. F. Chu, M. Šob, R. Siegl, T. E. Mitchell and S. P. Chen, Phil. Mag. B, **70**, 881 (1994).
42. A. H. Omenci, F. Chu, S. P. Chen, D. J. Thoma, J. Wills, and R. C. Albers, to be published.
43. F. Chu, D. J. Thoma, Y. He, T. E. Mitchell, S. P. Chen, and J. H. Perepezko, in this volume.